Proceedings of the 48th National Conference on Fluid Mechanics and Fluid Power (FMFP)
December 27-29, 2021, BITS Pilani, Pilani Campus, RJ, India.

FMFP2021–08–102

Blood Flow Analysis Through Bifurcated and Stenosed Coronary Artery

Nagaharish G N[1], Abdulrajak Buradi[1*], Prahlad V Deshpande[1], Nitesh Basavaraj Hallad[1], Madhusudhan A[1] and Bhaskor Jyoti Bora[2]

[1]Centre for Computational Fluid Dynamics, Mechanical Engineering Department, Nitte Meenakshi Institute of Technology, Yelahanka, Bangalore-560064, Karnataka, India.
[2]Energy Institute Bangalore, Centre of Rajiv Gandhi Institute of Petroleum Technology, Bangalore-560064, Karnataka, India
[*]Corresponding Author Email ID: arbnitk@gmail.com

ABSTRACT

Atherosclerosis is a very prominent disease in many countries these days. The detection of this disease has been difficult as the instruments required are very costly. Studies have been going on to find areas that are prone to the formation of stenosis. These works help us to understand and monitor these regions that are prone to the formation of stenosis. In this study, two models have been considered which are a patient-specific idealized model with a healthy model and a model with a 30% block. The analysis has been carried out using the Computational Fluid Dynamics (CFD) technique. It helps us in understanding the regions which are prone to the development of stenosis in the future. This study shows the velocity, pressure, and Wall Shear Stress (WSS) which helps us to see the flow behavior of blood in the laminar conditions with the Quemada viscosity model.

Keywords: Atherosclerosis, Computational Fluid Dynamics (CFD), Laminar Flow, Quemada viscosity model, Wall Shear Stress (WSS)

1. INTRODUCTION

Cardio Vascular diseases are one of the most increasing problems that lead to many deaths. These diseases mainly occur due to disturbances caused in the blood flow and particles that may enter our blood with oxygen which is responsible for the damage of the endothelial cells. The arteries are lined by a thin layer of epithelium made of Endothelial cells resulting in the formation of the endothelium. The endothelium has a high elastic nature. When the blood flows at high intensities through these arteries, the elastic nature of the endothelium helps to maintain the artery from collapsing on itself. This endothelial cell layer damage is initiated by different mechanisms like bacterial or viral infection, oxidative stress through abnormal regulation of reactive oxygen species, hypoxia, turbulent blood flow and shear stress, environmental irritants such as tobacco, and hyperlipidemia [1].

The coronary arteries are the blood vessels that are responsible for supplying the heart with oxygenated blood and nutrients [2,3]. Atherosclerosis is usually caused due to the low wall shear stress and flow disturbances due to the deposition of plague in the arteries [4, 5].

Hemodynamics and Computational Fluid Dynamics (CFD) are used for the better visualization of the flow disturbances caused in blood flow. Hemodynamics helps us to understand the behavior of blood flow and CFD helps us in visualizing the flow at different times. Several studies have shown that the blood flow in coronary artery bifurcations has given an insight into the diseases caused in coronary arteries [2, 6, 7].

The hemodynamic factors are affected due to the geometric parameters like a sudden change in the diameter due to stenosis, bifurcation, curvature, and tortuosity [8, 9]. The hemodynamic changes in the coronary arteries due to the buildup of plague are correlated with adverse clinical outcomes [10].
In this study, the Quemada viscosity model with laminar flow condition is used on a bifurcated healthy, and a 30% stenosed model. The velocity, pressure, and wall shear stress (WSS) of the blood flow have been studied.

2. METHODOLOGY

2.1 Coronary artery geometry with bifurcation and stenosis

The 3D model is designed using the Autodesk Fusion360 software. We have designed a 3D model of the blood artery with variable dimensions. Our design has been derived from a study conducted by Zaman N et.al. [11]. This design has been referred since it is patient-specific data from computer tomography angiography, that has been used to produce an idealized coronary artery model. We have taken two models, one is a healthy model, the second one has a stenosis of 30% blockage just after the first major bifurcation.

The total height from Inlet to Outlet 4 is 200 mm. The inlet has a diameter of 5 mm and Outlets 1 and 2 have 2 mm diameter. Outlet 3 has a diameter of 3.4 mm and outlet 4 has a diameter of 3.6 mm. All the design parameters shown in Table 1 remain the same for both the model. Model 2 has a 30% blockage after the major bifurcation 1 as shown in figure 2.

For each model, there are 3 zones (shown as circles in figure 1) that are marked which are considered for the study, in zone 1 the first bifurcation can be called the major bifurcation 1 and zone 2 is called the minor bifurcation. The zone 3 which is at the bottom is the major bifurcation 2.

S. Bhattacharyya and A. C. Benim (eds.), *Fluid Mechanics and Fluid Power (Vol. 2)*,
Lecture Notes in Mechanical Engineering, https://doi.org/10.1007/978-981-19-6970-6_2

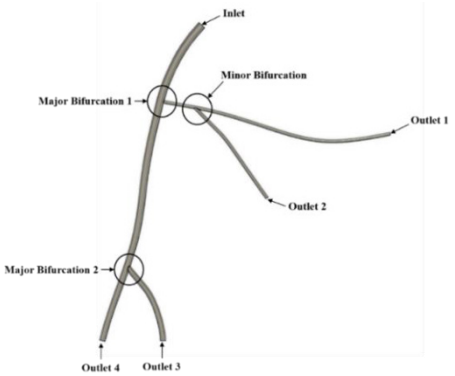

Figure 1: Coronary artery healthy model with different zones

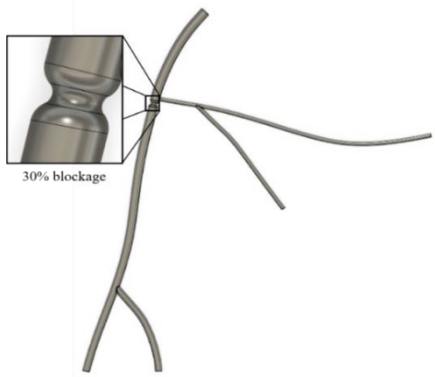

Figure 2: Coronary artery model with 30% blockage just after the major bifurcation 1

Table 1: Design parameters

Design Parameters	Values
Diameter at Inlet	5 mm
Diameter at Outlet 1	2 mm
Diameter at Outlet 2	2 mm
Diameter at Outlet 3	3.4 mm
Diameter at Outlet 4	3.6 mm
Inlet Area	19.635 mm^2
Outlet 1 Area	3.142 mm^2
Outlet 2 Area	3.142 mm^2
Outlet 3 Area	9.079 mm^2
Outlet 4 Area	10.179 mm^2
Major Bifurcation 1 angle	93°
Major Bifurcation 2 angle	58°
Minor Bifurcation 1 angle	35°

2.2 Equations governing the blood flow

The fluid flow always is bound by the continuity and momentum equation this implies that mass and momentum always conserved.

The following continuity and momentum equation can be expressed as:

Continuity Equation:

$$\frac{\partial \rho}{\partial t} + \rho\left(\frac{\partial u_x}{\partial x} + \frac{\partial u_y}{\partial y} + \frac{\partial u_z}{\partial z}\right) = 0 \quad (1)$$

Momentum Equation:

$$\rho\frac{\partial u_x}{\partial t} = -\frac{\partial p}{\partial x} + \frac{\partial \tau_{xx}}{\partial x} + \frac{\partial \tau_{yx}}{\partial y} + \frac{\partial \tau_{zx}}{\partial z} + \rho f_x \quad (2)$$

$$\rho\frac{\partial u_y}{\partial t} = -\frac{\partial p}{\partial y} + \frac{\partial \tau_{xy}}{\partial x} + \frac{\partial \tau_{yy}}{\partial y} + \frac{\partial \tau_{zy}}{\partial z} + \rho f_y \quad (3)$$

$$\rho\frac{\partial u_z}{\partial t} = -\frac{\partial p}{\partial y} + \frac{\partial \tau_{xz}}{\partial x} + \frac{\partial \tau_{yz}}{\partial y} + \frac{\partial \tau_{zz}}{\partial z} + \rho f_z \quad (4)$$

The simulation has been done using the Laminar viscous model. Quemada Viscosity Model UDF has been used for the simulation. The Quemada Viscosity as stated in [12], the blood viscosity is related to structure parameter (u) and RBC volume fraction ($\boldsymbol{\varepsilon}$). This is given by:

$$\mu = \mu(\alpha\boldsymbol{\varepsilon}) = \mu_{\boldsymbol{a}}\frac{\mathbf{1}}{(1-0.5u\varepsilon)^2} \quad (5)$$

where, μ = Viscosity

μ_a = 0.00132 Pa s [13]

The structure parameter (u) is defined by:

$$u = \frac{u_0 + u_\infty\sqrt{\alpha^s/\alpha}}{1+\sqrt{\alpha^s/\alpha}} \quad (6)$$

Where, u_0, u_∞ and α^s are a function of $\boldsymbol{\varepsilon}$ [13,14].

2.3 Computational modelling

2.3.1 Computational mesh

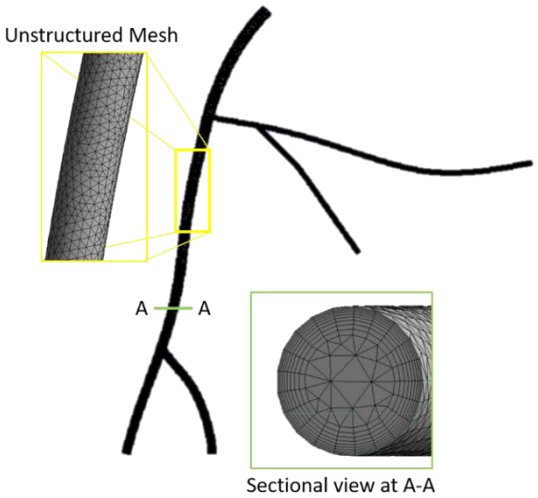

Figure 3: Computed mesh with a zoomed view of the cross section

The 3D model of the blood vessels is meshed using the Academic version of the ANSYS 19 software. The mesh is made for CFD and with medium unstructured (tetrahedron) meshes and there are 10 inflation layers given to the blood vessel walls with a smooth transition and transition ratio of 0.272. The inflation layer is added as our study requires a close look at the wall shear. The mesh has around 7,00,000 to 7,50,000 elements.

2.3.2 Mesh independent study

The mesh independent study has been done based on the precision of the results and the time taken for the computation. 3 meshes of one model have been considered, the elements of the first one ranging from 5,00,000 to 5,50,000. The second one has elements ranging from 7,00,000 to 7,50,000. The third mesh has over 10,00,000 elements. The test has been conducted by importing the mesh file into the FLUENT software and then the

tested for 10000 iterations The maximum values of velocity and wall shear stress.

Table 2: Mesh independent study values

Mesh Type	No. of Elements	Max. Velocity	Max. Pressure	Max. WSS
Coarse	598144	2.7	237.912	185.213
Medium	754101	2.7805	222.742	204.89
Fine	1000046	2.79707	220	209.312

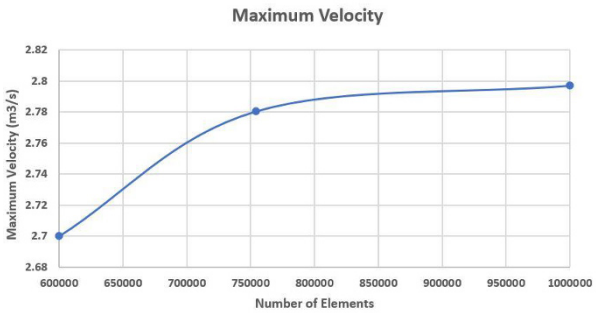

(a)

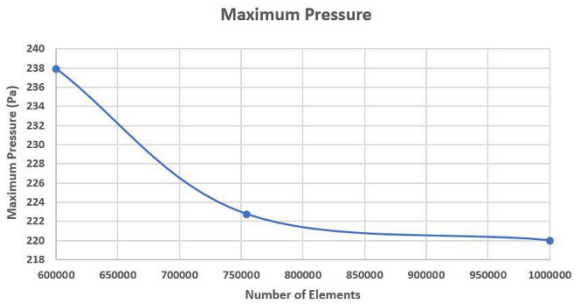

(b)

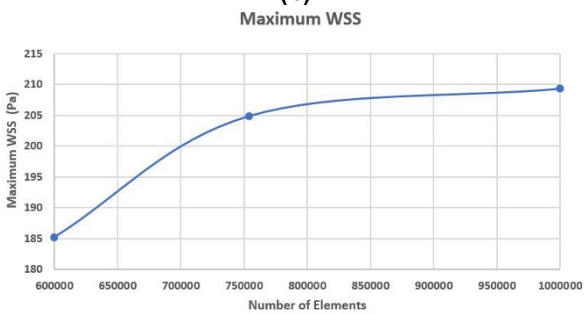

(c)

Figure 4: Graphs plotted for mesh independent study (a) Maximum velocity v/s No. of Elements (b) Maximum pressure v/s No. of Elements (c) Maximum WSS v/s No. of Elements

The above line graphs depict the difference in results obtained from the different number of mesh elements. The graph in Figure 4 (a) shows the maximum values of velocities, Figure 4 (b) shows the maximum pressure and Figure 4 (c) is the graph for the Maximum Wall Shear Stress obtained for the different meshes of the same model. The velocity obtained using the coarse mesh has given a very low value, but the computational time taken by this mesh was very less compared to the values and time taken by the other two meshes. The difference between the values obtained by medium mesh and a fine mesh is very minimal but the computational time taken by the fine mesh is very high due to the high number of elements when compared to the medium mesh. Therefore, the medium mesh range has been selected for our study since it gives very close values to that of the fine mesh, and also the computation time is also less compared to the fine mesh.

2.4 Boundary conditions

At the inlet, the blood density is set to 1060 kg/m^3 and the Quemada Viscosity models have been used. The velocity is an unsteady velocity UDF that has been interpreted into the software. The artery walls have been set to stationary wall conditions. The Outlets 1, 2, 3, and 4 have been set to Outflow condition. Figure 5 shows the Inflow velocity conditions. Each pulsating cycle is 0.75 seconds. The contours for the study have been taken at the 0.55s time step as the flow at this timestep is maximum.

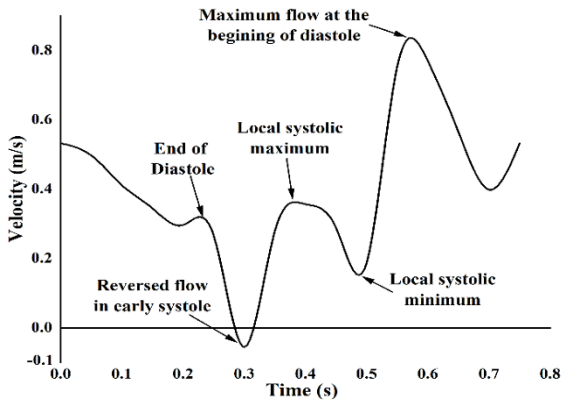

Figure 5: In-flow velocity profile for blood (plasma and RBC) during one pulsatile cycle [15]

2.5 Validation of the blood flow

The simulations are carried for water (Newtonian fluid) to find the accuracy of the present CFD simulations in a bifurcation T channel and compared the results with the numerical data [16] and experimental data [17] existing in literature for the bifurcation T channel. The geometry considered for the validation study consists of the main artery branch that breaks into two daughter arteries separated by 90^0 bifurcation angles. The length and width of the vessel are 30H and H for daughter and mother vessels. The 2D vessel geometry is used to perform the simulations for both cases. The 2D bifurcation vessel geometry is shown in Fig. The results of the velocity profile as shown in Figure 6 are obtained from the present CFD simulations are compared with available literature data. The velocity profiles shown by the red line are obtained by creating a line on the middle plane at a distance of 0.0005 m from the bifurcation. At the inlet, a parabolic velocity profile of Re = 496 is imposed for the blood flow analysis. The present CFD simulation results are in good agreement with the available literature data.

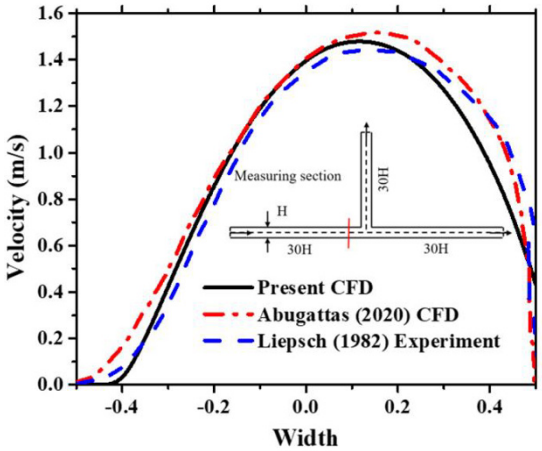

Figure 6: Validation of present CFD results with the computational data [16] and the experimental data [17] for Newtonian fluid flow at the bifurcation T channel at Re = 496.

3. RESULTS AND DISCUSSION

3.1 Influence of bifurcation and stenosis on velocity distribution

The above figures depict the velocity contours of the 2 models that are considered for the study. The simulation was done for three cardiac cycles to get the repeatable solution. Then the results of the second cardiac cycle are considered for analysing the various distribution and variations of different hemodynamic for different tortuous models. The velocity contour has been taken at the peak value of the unsteady velocity at 0.55 seconds.

Figure 7 (a) shows the healthy model, in major bifurcation 1, there is a high velocity in the first bifurcation which is with an angle of 93 degrees, this is due to the sudden change in the diameter of the fluid flow and also the high bifurcation angle. In the minor bifurcation, there are some regions of velocity. In the major bifurcation 2 of Figure 7 (a) slight recirculation zones are noticed at the outer wall surfaces. These regions of low velocities lead to recirculation which can lead to the damage of the endothelial layer which are the regions with high possibilities for stenosis development.

Figure 7 (b) shows the model with one stenosis of 30% blockage just after the first bifurcation. In this model, in the major bifurcation 1, it is seen that the velocity is high same as in Figure 7 (a), however, in the minor bifurcation of Figure 7 (b) it is observed that the recirculation region has reduced compared to the first model. This can be due to the presence of the stenosis just after the major bifurcation, the stenosis blocks the smooth flow in the major artery and this results in more flow into the bifurcated artery compared to the first model. Thereby, it can be noticed that fewer regions with low velocity in the minor bifurcation in Figure 7 (b). There is a momentary pressure increase due to the presence of stenosis. Due to the sudden decrease in diameter at the stenosis by 30%, this creates a recirculation zone just after the stenosis and the velocity in this recirculation region is very low. This region of recirculation with low velocity is prone to the damage of the endothelial cell layer and leads to the deposition of plague. In the major bifurcation 2 of the second model as observed in Figure 7 (b), it can be seen that the low-velocity region is shorter compared to the low-velocity zone length in Figure 7 (a). This is due to the increase in the velocity by the 30% blockage.

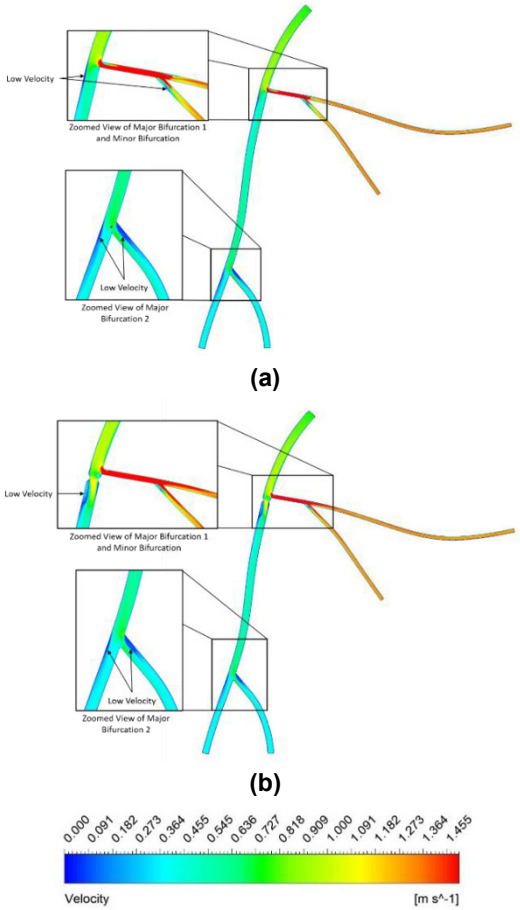

Figure 7: Velocity contours of (a) Healthy model (b) 30% blockage model at 0.55s timestep with the maximum flow

3.2 Influence of bifurcation and stenosis on WSS distribution

The tangential Force that is acting on the artery wall or the endothelial cell layer due to the flow of blood is known as wall shear stress (WSS). The WSS for the blood flow in the arteries is calculated using the relation:

$$\tau = \mu \frac{du}{dy} [6] \quad (7)$$

The above images show the WSS contour. The studies show that the regions where the WSS is less than 1.5 Pa are prone to the formation of stenosis. The regions with low WSS have a high recirculation or high oscillatory shear index (OSI). Higher the OSI higher the damage of the endothelial cells in the blood vessel. In figure 8 (a), it can be observed that in the region opposite to the first major bifurcation we see there is a very low WSS this region is one of the regions where the stenosis can start building up. This low WSS is because of the sudden bifurcation which is changing the flow direction partly. Moving

further down the artery, at the second major bifurcation at the lower half of the model, it is seen that the region away from the bifurcation has a very low WSS. Here, the bifurcation is more towards the center of the major flow which makes the flow to hit the bifurcation region and in the outer region there is vortex formation which is the region with WSS.

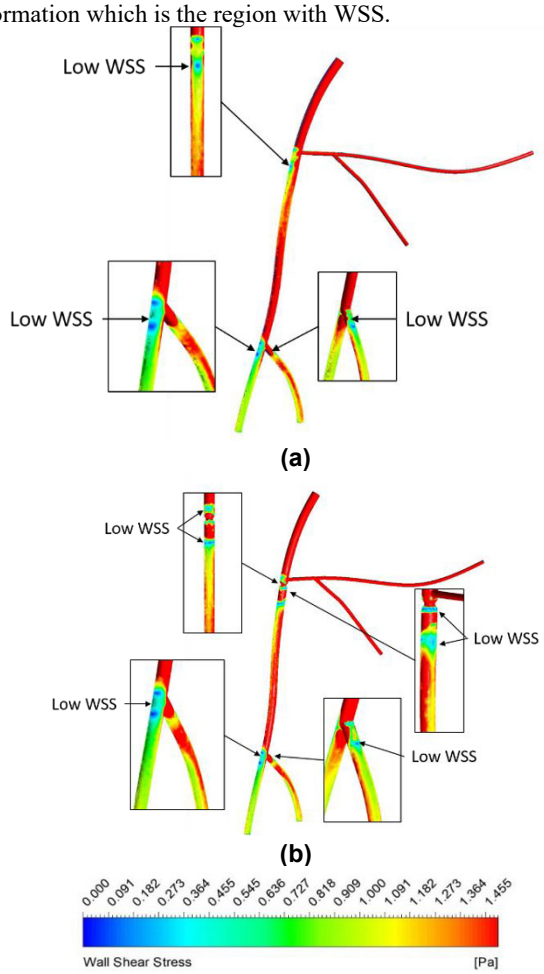

Figure 8: WSS contours of (a) Healthy Model (b) 30% blockage model at 0.55s timestep with the maximum flow

Figure 8 (b) shows the model having a 30% blockage just after the first major bifurcation here we can see the low WSS region just before and just after the stenosis. This contour agrees with the study done by A. Buradi, & A. Mahalingam[10] for the 30% stenosis condition. This is because of the sudden change in the diameter of the blood vessel which gives rise to a disturbance in the flow. Due to the stenosis, the area of cross-section reduces and this creates a low WSS region further down in the artery as seen in the figure. By the time the flow reaches the second major bifurcation, the flow is stable and flow behaves the same way as model 1 at the second major bifurcation.

3.3 Influence of bifurcation and stenosis on pressure distribution

The pressure contours shown in figure 9 (a) to (b) for the 2 models show the regions of very low pressures which can be at times very low that it can lead to damage in the blood vessel. Figure 9 (a) shows the pressure contour for a healthy blood vessel, here it is noticed that the pressure in the main artery is high but at the first major bifurcation as shown in the zoomed view there is the pressure drop and the pressure is very low at the bifurcation. This pressure drop is because of the sudden reduction in the diameter, and this region has a high velocity due to the change in diameter. At the second major bifurcation, there is no major change in the pressure.

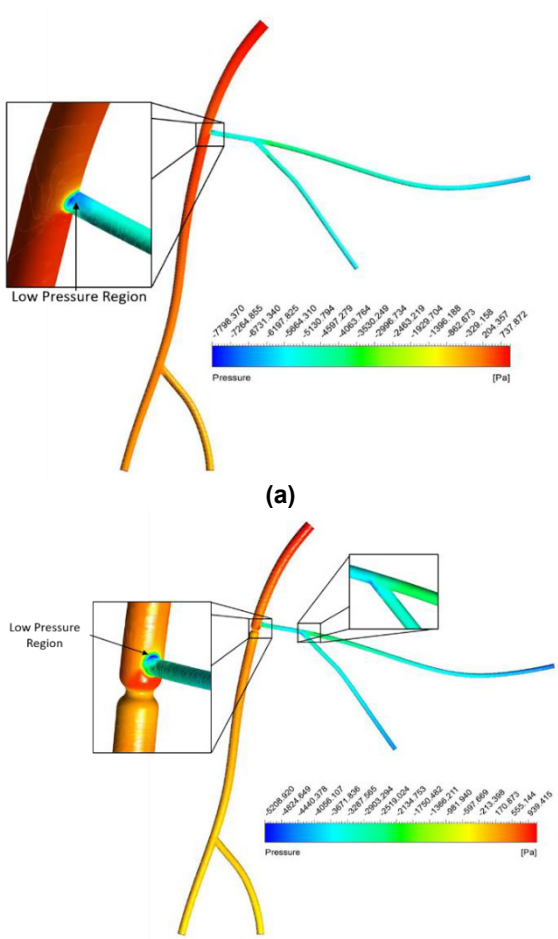

Figure 9: Pressure contours on wall of blood vessel of (a) Healthy model (b) 30% blockage model at 0.55s timestep with the maximum flow

In figure 9 (b), it can be observed that at the first major bifurcation, there is a pressure drop at the bifurcation. However, just above the stenosis, there is high pressure. In this high-pressure region, there is low velocity due to the recirculation created due to the change in the diameter. Furthermore, the pressure in the major artery is comparatively lower when compared to model 1 as depicted in figure 9 (a).

4. CONCLUSIONS

Cardio Vascular Disease (CVD) which is very dangerous and also gets detected mostly in very complicated situations makes it very dangerous for the patients. This study is based on

a patient-specific idealized model that is used to study the blood flow behavior with laminar flow condition and the Quemada viscosity model is used. The fluid (blood) is considered as a non-Newtonian fluid with an unsteady velocity UDF. The results show that in the healthy model the small regions with low velocity and Wall Shear Stress act as the initiation for the development of stenosis. Due to the low velocity and WSS, this region will have recirculation which is responsible for the damage of the endothelial cell layer which facilitates plaque accumulation resulting in the reduction of the flow area. The stenosis in the second model (30% stenosis) is considered in the region just after the major bifurcation 1 since it is observed that there is a region of low WSS in the first model (Healthy model) just after the major bifurcation 1. This results in the shift of the regions of low velocity and the low WSS to shift further below. The decrease in pressure will increase the velocity. Due to this, the flow will be directed in a particular direction which will cause recirculation in the other regions with low velocity and WSS as seen in figures 7(b) and 8(b).

NOMENCLATURE

f_x	Body force in x-direction	N
f_y	Body force in y-direction	N
f_z	Body force in z-direction	N
u_z	Velocity component in z-direction	m/s^2
u_x	Velocity component in x-direction	m/s^2
u_y	Velocity component in y-direction	m/s^2
μ	Viscosity	Ns/m^2
μ_a	Viscosity of plasma (0.00132 Pa s)	Pa s
α	Shear rate	s^{-1}
u	Structure Parameter	--
τ	Wall Shear Stress	Pa
ϕ	Coefficient of viscosity	Ns/m^2
$\frac{du}{dy}$	Velocity Gradient or Strain Rate	--

REFERENCES

1. R. Ross. Atherosclerosis—an inflammatory disease, New England journal of medicine, 340(2), 1999, pp. 115-126.
2. J. J. Asiruwa, A. M. Propst, and S. P. Gent, Assessing Near-Wall Hemodynamics of Blood Flow in the Left Anterior Descending Segment of the left Coronary Artery using Computational Fluid Dynamics, ASME International Mechanical Engineering Congress and Exposition, Vol. 58363, 2017, p. V003T04A023.
3. A. Mahalingam, U.U. Gawandalkar, G. Kini, A. Buradi, T. Araki, N. Ikeda, A. Nicolaides, J.R. Laird, L. Saba, and J.S. Suri, Numerical analysis of the effect of turbulence transition on the hemodynamic parameters in human coronary arteries, Cardiovascular Diagnosis and Therapy, 6(3), 2016, p.208.
4. C. G. Caro, J. M. Fitz-Gerald, and R. C. Schroter, Atheroma and arterial wall shear-Observation, correlation and proposal of a shear dependent mass transfer mechanism for atherogenesis, Proceedings of the Royal Society of London, Series B. Biological Sciences, 177(1046), 1971, pp. 109-133.
5. A. Buradi, and A. Mahalingam, Numerical Analysis of Wall Shear Stress Parameters of Newtonian Pulsatile Blood Flow Through Coronary Artery and Correlation to Atherosclerosis, In Advances in Mechanical Engineering, Springer, Singapore, 2020, pp. 107-118.
6. H. Nordgaard, A. Swillens, D. Nordhaug, I. Kirkeby-Garstad, D. Van Loo, N. Vitale, and L. Lovstakken. Impact of competitive flow on wall shear stress in coronary surgery: computational fluid dynamics of a LIMA–LAD model, Cardiovascular Research, 88(3), 2010, pp. 512-519.
7. A. Buradi, S. Morab, and A. Mahalingam, Effect of stenosis severity on shear-induced diffusion of red blood cells in coronary arteries, Journal of Mechanics in Medicine and Biology, 19(05), 2019, p.1950034.
8. D. D. Duncan, C. B. Bargeron, S. E. Borchardt, O. J. Deters, S. A. Gearhart, F. F. Mark, and M. H. Friedman, The effect of compliance on wall shear in casts of a human aortic bifurcation. 1990
9. A. Buradi, and A. Mahalingam, Impact of coronary tortuosity on the artery hemodynamics, Biocybernetics and Biomedical Engineering, 40(1), 2020, pp.126-147.
10. A. Buradi, & A. Mahalingam, Effect of stenosis severity on wall shear stress based hemodynamic descriptors using multiphase mixture theory. J. Appl. Fluid Mech, 11(6) , 2018, pp. 1497-1509.
11. N. Zaman, M. Ferdows, M. A. Xenos, K. E. Hoque, and E. E. Tzirtzilakis. Effect of angle bifurcation and stenosis in coronary arteries: An idealized model study, BioMed Res. J, 4(3), 2020, pp. 214-228.
12. D. Quemada, Rheology of concentrated disperse systems II. A model for non-Newtonian shear viscosity in steady flows, Rheologica Acta, 17(6), 1978, pp. 632-642.
13. C. G. Caro, T. J. Pedley, R. C. Schroter, and W. A Seed, The mechanics of the circulation. Cambridge University Press. 2012
14. G.R. Cokelet, The rheology and tube flow of blood, In Handbook of Bioengineering. New York: McGraw-Hill, 1987 [Chapter 14].
15. R.M. Berne and M.N. Levy, Cardiovascular physiology, Mosby, 1967.
16. C. Abugattas, A. Aguirre, E Castillo, & M Cruchaga, Numerical study of bifurcation blood flows using three different non-Newtonian constitutive models. Applied Mathematical Modelling, 88, 2020, pp. 529-549.
17. D. Liepsch, S. Moravec, A. K. Rastogi, and N. S. Vlachos, Measurement and calculations of laminar flow in a ninety-degree bifurcation, Journal of biomechanics, 15(7), 1982, pp. 473-485.